

aerosol optical depth of 0.4) over the tropical northern Indian Ocean. In cloudy conditions over the ocean, the sea-salt aerosols partly offset the TOA positive forcing (heating) by soot aerosol, while complementing the surface forcing. The sea-salt aerosol has a significant role in determining the TOA radiance measured by satellites and hence algorithms for retrieving the aerosol properties from satellites should have wind speed as input to account for the changes in aerosol chemical composition with wind speed. Since sea-salt absorbs in the infrared, the retrieval of SST from satellite data (IR brightness temperature) should take into account the sea-surface wind-speed changes.

1. Moorthy, K. K., Satheesh, S. K. and Krishna Murthy, B. V., *J. Geophys. Res.*, 1997, **102**, 18827–18842.
2. Fitzgerald, J. W., *Atmos. Environ.*, 1991, **25**, 533–545.
3. Lovett, R. F., *Tellus*, 1978, **30**, 358–364.
4. Hoppel, W. A., Fitzgerald, J. W., Frick, G. M. and Larson, R. E., *J. Geophys. Res.*, 1990, **95**, 3659–3686.
5. Ramanathan, V. *et al.*, *J. Geophys. Res.*, 2001 (in press).
6. Satheesh, S. K. and Ramanathan, V., *Nature*, 2000, **405**, 60–63.
7. Satheesh, S. K. *et al.*, *J. Geophys. Res.*, 1999, **104**, 27421–27440.

8. Shaw, G. E., Reagan, J. A. and Herman, B. M., *J. Appl. Meteorol.*, 1973, **12**, 374–380.
9. Hess, M., Koepke, P. and Schult, I., *Bull. Am. Meteorol. Soc.*, 1998, **79**, 831–844.
10. Podgorny, I. A., Conant, W. C., Ramanathan, V. and Satheesh, S. K., *Tellus*, 2000, **B52**, 947–958.
11. Breigleb, B. P., Minnis, P., Ramanathan, V. and Harrison, E., *J. Climat. Appl. Meteorol.*, 1986, **25**, 214–226.
12. Jayaraman, A., Lubin, D., Ramachandran, S., Ramanathan, V., Woodbridge, E., Collins, W. and Zalpuri, K. S., *J. Geophys. Res.*, 1998, **103**, 13827–13836.
13. Podgorny, I. A. and Ramanathan, V., *J. Geophys. Res.*, 2001 (in press).
14. Heintzenberg, J. *et al.*, *Beitr. Phys. Atmos.*, 1997, **70**, 249–263.

ACKNOWLEDGEMENTS. I thank Prof. J. Srinivasan, Centre for Atmospheric and Oceanic Sciences, Indian Institute of Science, Bangalore and Dr K. Krishna Moorthy, Space Physics Laboratory, Thiruvananthapuram for valuable suggestions and discussion. I also thank Prof. V. Ramanathan, Centre for Atmospheric Sciences, Scripps Institution of Oceanography, San Diego for providing the radiative transfer model. Thanks are also due to Ms Vidyumala for providing the NCEP wind data.

Received 18 August 2001; revised accepted 10 October 2001

# Impact of Deccan volcanism on deep crustal structure along western part of Indian mainland and adjoining Arabian Sea

A. P. Singh

National Geophysical Research Institute, Uppal Road, Hyderabad 500 007, India

To understand the magmatic processes originating in the deep mantle and their impact on the lower crustal level, the conspicuous gravity anomalies observed over the western part of Indian mainland and contiguous Arabian Sea were modelled, integrating the available seismic information. The unified 2D and subsequent 3D density modelling of the Narmada–Tapti region suggests a 15–20 km thick high-density ( $3.02 \text{ g cm}^{-3}$ ) accreted igneous layer at the base of the crust. The thickness of this layer varies from about 8 km near Multai to about 16 km beneath the central part and about 24 km beneath Navsari in the westernmost part of the Narmada–Tapti region. Similarly, a 7–11 km thick accreted igneous layer characterizes the Eastern Basin, including the Laxmi Ridge (LR) in the northeastern Arabian Sea. Thick-

ness of this layer varies from about 4 km beneath the northwestern part to about 11 km beneath the central part of the LR. The extension of this layer towards the southeast and ultimate connection with the Chagos–Laccadive Ridge makes the western boundary of the magmatic crustal accretion along the west coast of India. The Konkan Coast, further down south, is also characterized by a ca. 3 km thick and about 40 km wide accreted igneous layer at the base of the crust along the coastline. It is suggested that this widespread magmatic underplating along the western part of Indian land mass and adjoining Arabian Sea is the imprint of the Deccan magmatism caused by the deep mantle plume, when the northward migrating Indian plate passed over the Reunion hot spot.

THE western part of Indian mainland and adjoining Arabian Sea distinguishes itself distinctly from its counterpart in the east. The region suffered most in the period after the break-up of Gondwanaland. During this

time it passed through an extremely dynamic phase, marked by an extensive plate reorientation and massive volcanism (Figure 1). Several micro-continents such as the Madagascar and the Sechelles-Mascarene block may have existed along the west coast, before being broken away from the mainland. Several hidden tectonic features

e-mail: apsingh\_ngri@yahoo.com

and complex geophysical signatures further characterize the region. The West Coast fault (WCF), the Narmada–Tapti rift system (NTR), the Cambay graben (CG), and the triple junction (TJ) are a testimony of its intense inner dynamics. Conspicuous concentration of positive gravity anomalies surrounding the TJ<sup>1</sup>, a string of hot springs oriented north-south between latitude 10 and 20°N (ref. 2) and the locus of internal current concentration along the west coast<sup>3</sup> reflect its abnormal crustal structure and thermomechanical behaviour. The radial drainage pattern together with the rifted crest shows a mantle updoming in the Gulf of Cambay region<sup>4</sup>. In the given circumstances, plume-associated TJ is the most accepted hypothesis for the present-day configuration of the west-coast mega-structure encompassing the Gulf of Cambay region<sup>5</sup>. Surface expression of the proposed plume is the Deccan flood basalt on the western part of Indian mainland. Around 65 MaBP, when the Indian subcontinent passed over the Reunion hot spot (mantle plume), the crust opened on the west coast of India and produced one of the largest flood basalt provinces on the earth's surface<sup>6–8</sup>.

Evidently an event of such magnitude must have had a profound influence on the crustal evolution, including the present-day configuration of the continental lithosphere. It has been suggested that igneous intrusion at the base of the crust may underlie all shallow flood basalts<sup>9</sup>. The western part of Indian land mass and adjoining Arabian Sea is no exception.  $V_p$  velocities of 7.2–7.5 km s<sup>-1</sup>, a typical seismic signature of such magmatic layers, are observed in the region<sup>10</sup> and suggest a crustal accretion in the CG. Recently, Coffin and Eldholm<sup>11</sup>, Raval<sup>12</sup>, and Kaila and Sain<sup>13</sup> have conjectured magmatic intrusion even beneath the various parts of the west-coast mega-structure. An endeavour is therefore made to delineate the expected crustal accretion at the base of the crust beneath the region. Emphasis was given to lower crustal parts, which are most significant for geodynamic models and where the impact of Deccan magmatism is most relevant. The inferred structure is then used to elucidate an integrated geodynamical evolutionary model based on the viscosity structure of the pre-rift lithosphere.

### Narmada–Tapti region

The Narmada–Son lineament (NSL) is the most conspicuous linear feature on the geological map of the west-central India (Figure 2). The NTR, westernmost part of the NSL, is covered by a thick pile of lava flows and characterized by several hidden tectonic structures and complex geophysical signatures. It is generally assumed that dyke swarms centred on a hot spot feed the plume-associated continental flood basalts. When a mantle plume or magma flows along pre-existing lithospheric weak zones, dykes may propagate parallel to the weak zones.

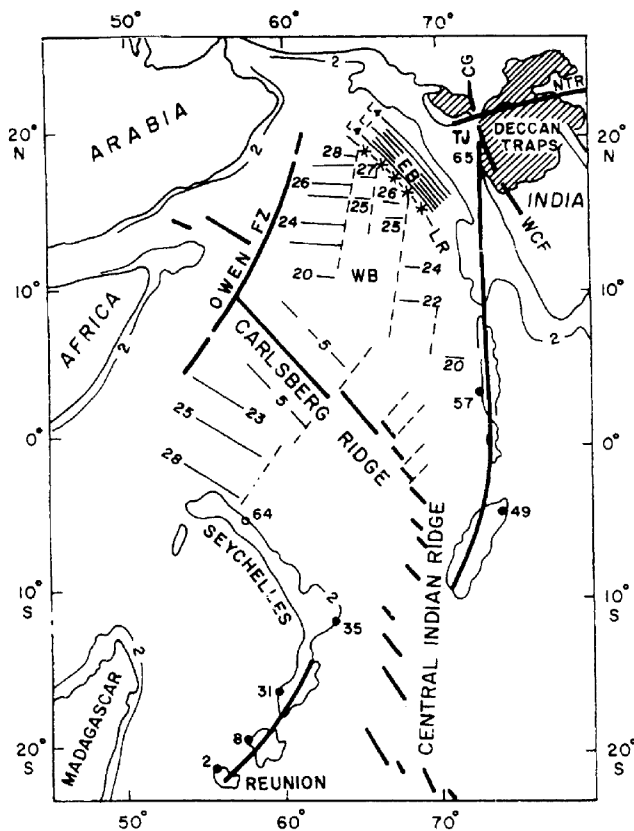


**Figure 1.** Present configuration of the western part of Indian mainland and adjoining Arabian Sea with the location of Madagascar, Seychelles–Mascarene block, Laxmi Ridge, Deccan Traps and the trail of the volcanic ridges and islands left by the Reunion plume as it migrated away from its initial position under India. Figures along the trail show the average age of the rocks in Ma. NTR; Narmada–Tapti region; CG, Cambay graben; TJ, triple junction in the Gulf of Cambay; WCF, West Coast fault; EB, Eastern Basin; WB, Western Basin; LR–Laxmi Ridge (modified after White and McKenzie<sup>9</sup>).

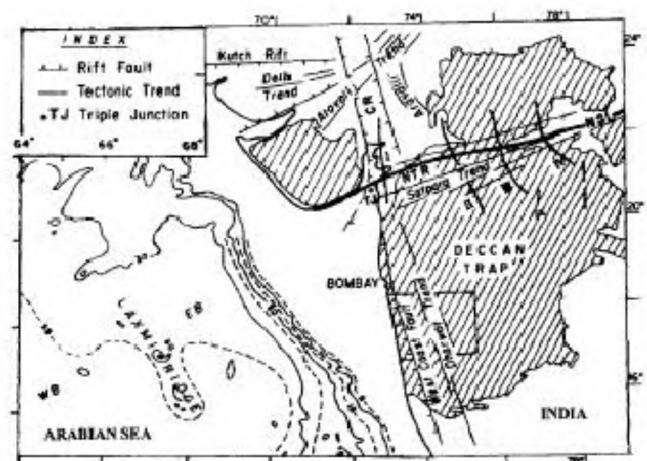


**Figure 2.** Pre-Cambrian trends and tectonic map of the western part of Indian mainland and bathymetric map of the adjoining Arabian Sea. Also shown are the four DSS profiles across the NTR and the study area of the Konkan coast marked just below Mumbai. Bathymetric map (counters in hundreds of metres at 500 m interval) of the northeastern Arabian Sea (after Naini and Talwani<sup>23</sup>) shows the LR, the EB and the WB.

The NTR and the west coast of India are full of dykes oriented in the respective direction. Field study shows that the frequency of dykes decreases from west to east along the NSL (ref. 14). Auden<sup>15</sup>, studying these dykes, suggested NSL to be a zone of crustal upwarping through which the Deccan lava intruded. A domal upwarping observed along the NSL with small dips along the limbs is believed to be responsible for the eruption of Deccan traps. The aeromagnetic anomaly map of the NSL further supports the belief of the geologists that a large area along the NSL served as channels through which fissure mode of lava eruption took place.

The Bouguer anomaly (BA) map of the NTR is characterized by a broad relative gravity high, aligned in the E-W direction between the rivers Narmada and Tapi (Figure 3). This gravity high has an average value of  $-25$  mGal compared to  $-40$  to  $-60$  mGal in the surrounding areas, and remains flat to the regional values approximately along the course of the rivers. The Navsari gravity high, with a maximum value of  $40$  mGal, forms the western extension of this linear gravity high. Another more local relative gravity high near Multai attains a peak value of  $-20$  mGal. To the east, the relative gravity high is interrupted by a NNW-SSE trending gravity low over Pachmarhi. This gravity low is perhaps the north-western extension of the Godavari graben.

The broad relative gravity high, associated with the Satpura mountains is in itself an anomalous feature, since the high region is expected to have a BA low due to the expected compensation of the topography. On the basis of the qualitative study of the BA along the NSL, Qureshy<sup>16</sup> concluded that the anomaly indicates a horst-type structure in which the crustal upliftment was associated with the movement due to incorporation of material from the upper mantle into the crust. The oval-shaped positive gravity anomaly over Navsari was ascribed to emplacement of high-density basic material raised from the mantle or an accumulation of large volumes of basic material around basic volcanic centres. In the realm

of Deccan magmatism, it presumably indicates a locus of volcanic activity. In fact, a similar anomaly over Mumbai coast is already ascribed as one of the fossil conduit pipes responsible for the Deccan magma evolution<sup>17</sup>.

The relative positive gravity anomaly of nearly  $100$  km in width and extending over a length of about  $600$  km provides an ideal condition for its two-dimensional examination. Integration of gravity modelling with the deep seismic sounding (DSS) profiles provides an excellent tool to quantify the deep crustal structures, where our knowledge is otherwise inadequate. To quantify the causative body for referred gravity anomaly, four DSS profiles in the NTR, viz. (I) Mehmabad–Billimora, (II) Thuadara–Sindad, (III) Ujjain–Mahan, and (IV) Khajuria kalan–Pulgaon were combined along the trend of BA by Verma and Banerjee<sup>18</sup>. They found that the broad relative gravity high was neither explained by the exposed geological features nor by the thickness variations of the different crustal layers and the Moho undulations beneath the Satpura mountains. In order to satisfy the observed BA, they introduced high-density intrusive material at mid-crustal levels, without giving any plausible explanation. On the other hand, Coffin and Eldholm<sup>11</sup> have assumed the presence of a lower crustal body. A fresh attempt was therefore made to arrive at a more comprehensive density model of the intrusive body beneath the region, integrating all the available seismic information<sup>19,20</sup>.

Along Profile-I, the anomalously high  $V_p$  layer ( $7.2$ – $7.4$  km s<sup>-1</sup>) is observed at the base of the crust all along the profile. Its top surface varies from about  $10$  km towards south to about  $23$  km towards north. The Moho was found to be deepest in the Jambusar–Broach graben occurring at  $38$ – $40$  km. In the northern region, it rises to  $32$  km near Mehmabad, whereas in the southern region it rises to less than  $25$  km near Billimora. Along Profile-II the high  $V_p$  layer at the base of the crust is not directly shown, but the interval velocity function along the profile infers its presence. In the depth range of  $27$ – $32$  km, an

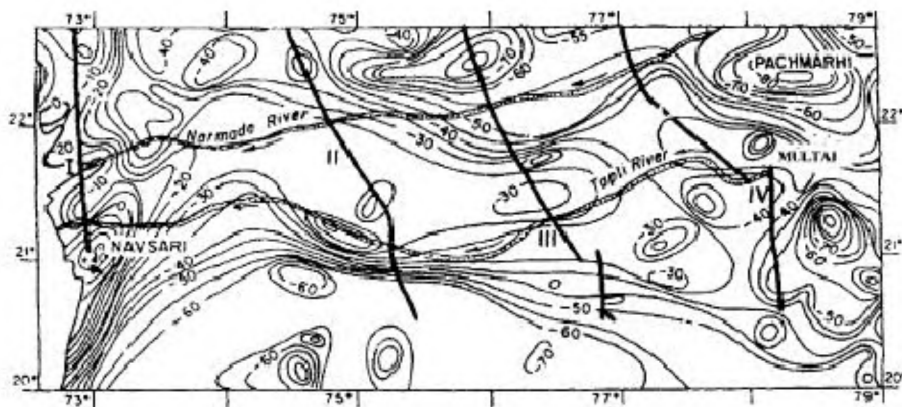


**Figure 3.** Bouguer anomaly map (in mGal) of the NTR (after Verma and Banerjee<sup>18</sup>) along with the DSS profiles and the course of the rivers Narmada and Tapi.

intermediate boundary with a velocity contrast was recognized. The Moho depth was found to vary from 38 to 43 km along the profile. It shows a gentle upwarp, with a relief of about 2 km in the region between the rivers Narmada and Tapi. Along Profile-III the velocity–depth function clearly indicates a  $V_p$  of 7.0–7.3 km s<sup>-1</sup> around 25–30 km depths. A thickening of crust below 37 km depth is observed in this region. The Moho depth was delineated in some parts of Profile-IV in the depth range of 34–40 km. No indication of high  $V_p$  layer at the base of the crust was found<sup>10</sup>. It might be too thin to be detected in accordance with the decreasing magmatic activity towards the east.

The shallow structural features were neither of interest nor was it appropriate to decipher on such a large scale in the absence of detailed geological/geophysical information. Hence the effect of the shallow crustal features was first adequately removed from the observed BA. Separation of gravity field originating from different source horizons is a vital subject in gravity interpretation. It has been proposed to use upward continuation as a sub-optimum filter for extraction of the field associated with sources below a certain depth<sup>21</sup>. The optimum filter for the extraction of the field associated with sources below a certain depth ( $Z_0$ ) is the upward continuation to the height ( $2Z_0$ ) above the measurement plane. A thickness of 15 km for the horizontal layer representing the upper crust was chosen and the observed BA map was subjected to the upward continuation to a height of 30 km, for extraction of the field associated with sources below 15 km depth (Figure 4). This filtered component of the BA was then used for the interactive forward gravity modelling developed by Götze and Lahmeyer<sup>22</sup>. The DSS study provided the necessary *a priori* information to well-constrain the initial 3D density model of the anomalous layer. Appropriate density values such as 2.87, 3.22 and 3.02 g cm<sup>-3</sup> are attributed to the lower crust, the upper mantle and the anomalous lower crustal layer, respectively and were held constant during the modelling. Except in the southwestern part of the region, the computed gravity values with minor adjustments in the subsurface geometry matched fairly well with the

filtered BA. The calculated gravity values for the given structure of the anomalous layer together with an up-warped Moho in the southwestern part of the region did not conform well to this part of the filtered BA. In contrast, upper and lower boundaries of the anomalous layer in the southwestern region were therefore suitably varied to match the anomaly. Care was, however, taken that the depth to the interfaces was compatible with the adjoining regions. The resulting 3D configuration of the anomalous layer lying above ~40 km deep Moho is shown in Figure 5. It clearly depicts the anomalous layer at the base of the crust whose thickness decreases gradually towards the east. Its thickness varies from 8 km near Multai to about 16 km in the central part of the region. A thickness of about 24 km below the Navsari gravity high is another local but prominent feature of the layer.

### Laxmi Ridge

Laxmi Ridge (LR) is the most conspicuous but least studied aseismic ridge of the adjoining Arabian Sea (Figure 2). It consists of isolated submarine structural highs of about 100 km in width and runs over a length of approximately 700 km. It divides the northeastern Arabian Sea into two crustal provinces. The area between the western end of the LR and the continental shelf of India is referred to as the Eastern Basin (EB). The area west of this region up to the mid-oceanic ridge is called the Western Basin (WB). Contrary to normal oceanic crust of ~11 km in the WB, a quasi-continental oceanic structure with a thickness of ~17 km is reported in the EB. A semi-oceanic crustal thickness of ~21 km, with an anomalous velocity of 7.15 km s<sup>-1</sup> and above at the base of the crust<sup>23</sup>, are the unique characteristics which make the LR more complex. Naini and Talwani<sup>23</sup>, Kolla and Coumes<sup>24</sup>, and Pandey *et al.*<sup>25</sup> believe that the crust underneath the EB is a transitional type, while Bhattacharya *et al.*<sup>26</sup>, and Singh<sup>27</sup> consider the crust to be oceanic in nature, formed by seafloor spreading.

Contrary to other aseismic ridges, the unusual crustal structure of the LR is further complicated by a negative

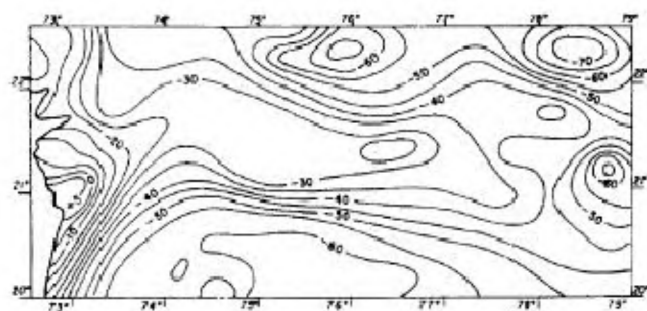


**Figure 4.** Thirty kilometre upward continued Bouguer anomaly map (in mGal) of the NTR.

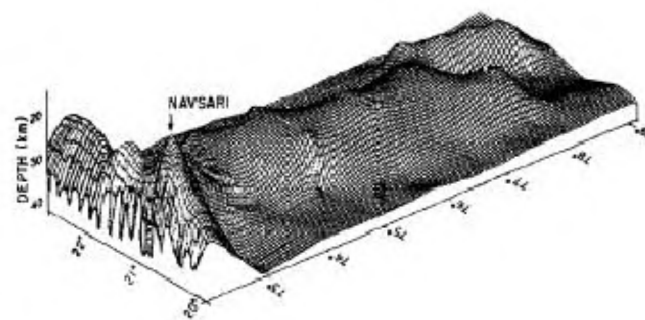


**Figure 5.** 3D configuration of the accreted igneous layer at the base of the crust beneath the NTR. Depths are in km from the surface.

free-air gravity anomaly observed over it (Figure 6). The low has an extreme value of  $-50$  mGal. The anomalies to the west of the gravity low are of a diffused nature, perhaps signifying normal oceanic crust devoid of any appreciable physical and compositional changes in this part. The free-air anomalies near the shelf edge seem to be influenced by the 'edge effect'. However, the negative gravity anomaly over the LR is far enough from the Indian continental margin to be largely unaffected by the continental gravitational 'edge effect'. Therefore, the gravity field over the ridge axis is believed to be affected only by the ridge and its compensating mass. Liu *et al.*<sup>28</sup> analysed a similar negative gravity anomaly over  $85^{\circ}\text{E}$  Ridge in the Bay of Bengal and ascribed the presence of crustal root to regional flexural compensation due to sediment loading. However, in case of the LR, the load due to an extremely thin sedimentary column ( $0.5$  km) would be well supported by the lithosphere, causing no flexure. A gravity low of  $-30$  to  $-40$  mGal with a wavelength of  $200$  km found over the LR, is also similar both in magnitude and in wavelength to that observed over relatively slow-spreading centres, both active and extinct<sup>29</sup>. However, the cited spreading centres have definite magnetic signatures associated with them. In contrast, the magnetic lineations in the EB rule out the possibility of the LR being an extinct spreading centre (Figure 1). The extinct spreading centre (L1) lies somewhat to the east of the LR<sup>26</sup>. The anomalous gravity low over the LR therefore needs a more comprehensive explanation.

The seismic information reveals a normal oceanic crust about  $11$  km thick in the WB. However, apart from the

other normal crustal columns an anomalous layer of velocity  $7.15\text{ km s}^{-1}$  and above was delineated at the base of the crust beneath the entire EB, including the LR. Thickness of this anomalous layer was, however, not well established. Assuming a velocity of  $8.2\text{ km s}^{-1}$  for the lower layer, Naini and Talwani<sup>23</sup> estimated the average minimum depth to Moho under the ridge axis to be greater than  $21$  km. The seismic information provided the well-constrained geometry of the initial 3D density model of the LR crust/mantle system. A density of  $3.02\text{ g cm}^{-3}$  corresponding to the velocity of  $7.2\text{ km s}^{-1}$  is again assigned to the transitional layer. This results in a negative density contrast of  $-0.28\text{ g cm}^{-3}$  with respect to an upper mantle density of  $3.30\text{ g cm}^{-3}$ . Trusting the above density values and geometry of the upper crustal layers, the least constrained crust/mantle interface was modified with minimum necessary adjustments in order to match the computed gravitational attraction with the observed free-air anomalies. The resulting 3D configuration of the crust/mantle interface (Moho) from the mean sea level is shown in Figure 7. It clearly depicts a normal crust of about  $11$  km thickness (with no transitional layer) in the WB. The most characteristic feature of the 3D density model is the thickened crust not only beneath the ridge axis, but extending in the entire EB. Thickness of the crust/mantle interface (Moho) with the transitional layer beneath the LR decreases gradually towards the NW. Its total thickness from mean sea level varies from  $15$  km beneath the NW to about  $22$  km beneath the central part of the ridge axis. Its continuation further into the south-eastern direction is another prominent feature of the LR. About  $6$ – $11$  km thick transitional layer in the EB, including the LR lying between  $11$  km (shown by dashed line in Figure 7) and the Moho depths is inferred again as the same anomalous layer at the base of the crust.

### Koyna coastal region

A thick but more or less flat pile of Deccan flood basalt covers this region, which tapers down towards the east

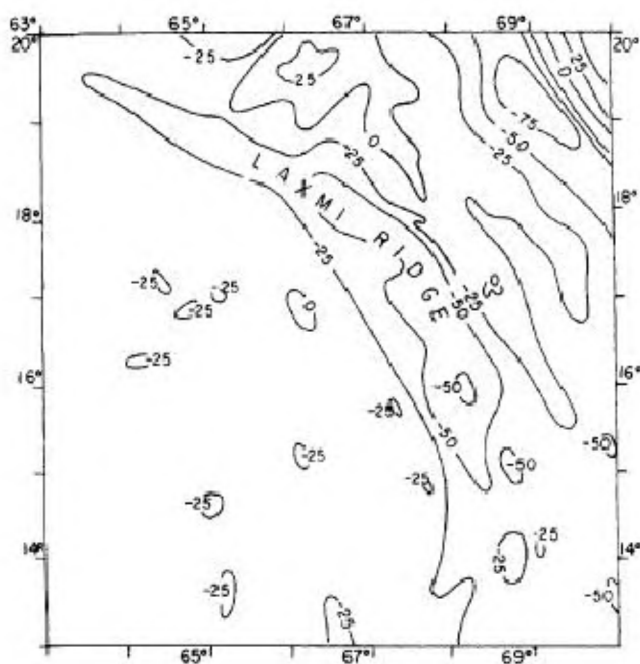


**Figure 6.** Free-air anomaly map (in mGal) of the LR (after Naini and Talwani<sup>23</sup>).

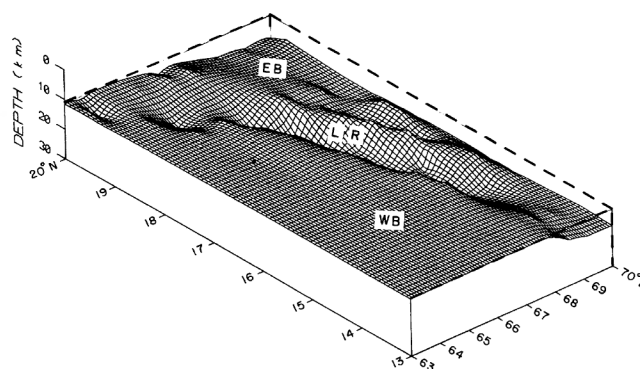


**Figure 7.** 3D structure of the crust/mantle interface (Moho) of the study area. Below  $11$  km from the mean sea level (marked by dashed line) in the EB, including the LR is the accreted igneous layer.

(Figure 2). The gravity anomaly map of the Koyna coastal region and the adjoining Arabian Sea along with the two DSS profiles available in the Konkan coastal region are shown in Figure 8. A significant feature of the map are some broad linear highs and lows parallel to the coast. The BA over the continental part is predominantly negative, whereas the free-air anomaly over the oceanic region is somewhat positive in nature. The BA over the continental part varies from  $-40$  to  $-110$  mGal. In contrast, the free-air anomaly over the oceanic region increases and attains a value of  $25$  mGal.

A comparison of the gravity anomaly with the thickness of the surface flood basalts shows no correlation, except for the general N-S trend. The pronounced BA low of about  $-110$  mGal located over the Mahad-Bhor-Koyna-Karad region is interpreted by Krishna Brahman and Negi<sup>30</sup> as being due to the presence of a rift valley concealed below the Deccan traps. In contrast, another interpretation is that the anomaly has deep-seated causes, being due to subsidence within the deep crustal and mantle layers<sup>31-33</sup>. Interestingly, the region is also characterized by a belt of negative Airy isostatic anomaly ranging from  $-40$  to  $-70$  mGal (ref. 1). This feature extends from the southern tip of India to a point north of Mumbai and a portion of it falls even outside the Western Ghats. A low BA/low Airy isostatic anomaly in general indicates a thicker than normal crust beneath the region. Intuitively, the expected downward deflection of various crustal columns beneath the region may be due to the vast spread Deccan volcanism together with the highly elevated Western Ghats along the coast. However, Subrahmanyam and Verma<sup>34</sup> hold that the isostatic anomaly does not seem to be controlled by topography, as it is spread over both the low-lying coastal plains and the elevated Western Ghats. According to Qureshy<sup>35</sup>, the low Airy isostatic anomaly may be due to an undissipated crustal root in the mantle and/or the local decrease in upper mantle density, probably caused by large mass transfer during the Deccan magmatism.

Another characteristic feature of the gravity map is the relative positive gravity anomaly at the coast with a gradual decrease towards the east. A contact of low-density granitic continental plate with a basaltic oceanic plate of high density in the Arabian Sea, could be an obvious explanation for the gravity gradient in such regions. A wide continental shelf, on the other hand, justifies the assumption that the part of the crust considered is continental and also that the linear trend is not due to the effect of the continental margin<sup>36</sup>. A quasi-continental crustal structural in the eastern basin of the adjoining Arabian Sea<sup>23</sup> further negates this possibility. Krishna Brahman and Negi<sup>30</sup> regarded it as being due to a major north-south fault zone. In contrast the relative positive anomaly, with a prolonged zone of high gravity gradient, is not likely to be caused by a fault, but is due to a massive crustal upwarp near the coastline<sup>32,37</sup>. It may be noted here that the linear N-S trend along the coastline is not a local feature on the BA map, as it extends northward along the Mumbai coast and joins the trend of the CG (ref. 1). The crustal upwarping, expected to be responsible for the anomaly, should therefore be a regional phenomenon in the entire coastal region. On the contrary, the positive gravity anomalies in nearby regions are interpreted as being due to a mass of high-density rock employed in the crust<sup>17,36,38</sup>. A possible southward extension of the emplaced crustal material may be lesser in amount seems to be a more plausible explanation for the referenced anomaly<sup>39</sup>.

The two available seismic profiles show the entire crustal structure with four distinct layers<sup>10</sup>. The thickness of the Deccan traps exposed on the surface varies from about  $1.6$  km along the coast to about  $0.6$  km towards the east. The basement lies directly beneath the Deccan traps. The mid-crustal level is characterized by a thin layer with strong reflectivity. The study further delineated a normal crust of about  $36-40$  km thickness in a major part of the region. The largest crustal thickness is at Koyna. Though the Moho was observed in most parts of the profiles, its

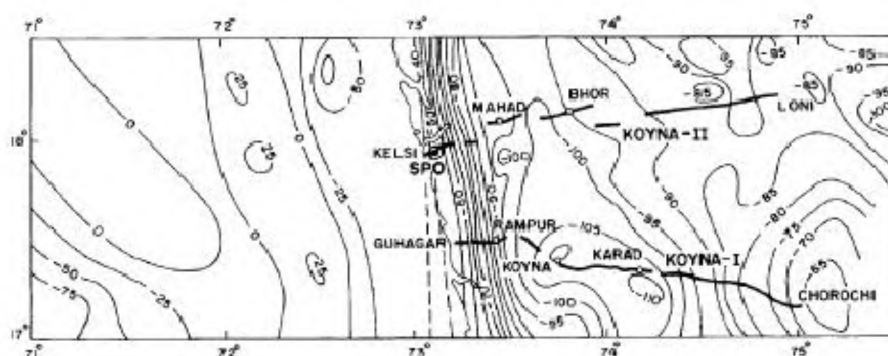


**Figure 8.** Gravity map (in mGal) of the Koyna coastal region and adjoining Arabian Sea with two DSS profiles Koyna-I and Koyna-II. Map consists of BA over the continental part (after Kailasam *et al.*<sup>31</sup>) and free-air anomaly over the oceanic region (after Naini and Talwani<sup>23</sup>).

extension towards the coastal region is an extrapolation with question marks<sup>10</sup>. With single-sided wide-angle reflection data and inadequate control from the oceanic region, it was not possible to delineate the Moho at this end point of the profiles. A spot value of about 30 km depth to the Moho boundary at the coast was therefore obtained from reciprocal recording of north-south shot points. Corroborating the gravity gradients, a wrap-up Moho may be obtained interpolating between the regions. No direct seismic signature of crustal accretion at the base of the crust beneath the region is indicated. The interval velocity function along these two profiles, however, infers its presence. As usual the lower crust is characterized by a  $V_p$  velocity of  $6.76 \text{ km s}^{-1}$ . Further down, the  $V_p$  velocity again increases, reaching a value of  $7.26 \text{ km s}^{-1}$  at the base of the crust. The synthetic seismogram modelling of crustal seismic record sections along these two profiles also revealed a 2 km thick transitional Moho at about 35.5 km depth<sup>40</sup>. In the realm of Deccan volcanism and locus of the plume path, this high-velocity transitional layer at the base of the crust is thought to be due to the intrusion of basaltic material from the mantle into the lower crust beneath this region<sup>13</sup>.

The observed BA along the DSS profiles is shown in Figure 9. The expected undulations in the deep crustal layers are well reflected in the broad regional features observed on the gravity profiles. The theoretical gravity values obtained for the given seismic sections as such are unexpectedly inconsistent with the observed gravity field. A highly warped-up Moho reaching a depth of about 30 km from the surface along the coastline, as suggested by the DSS studies, produces a relative positive gravity anomaly of a considerably higher magnitude than observed. In contrast, the calculated gravity values of the crustal structure with about 2 km thick transitional Moho between 35.5 and 37.5 km depth along the coast, where the crust/mantle transition zone was otherwise least constrained, were quite close to the observed BA. Keeping all the other parameters constant, the upper and lower boundaries of the transitional layer together with its density were therefore suitably adjusted to match the observed gravity anomaly. Care was, however, taken that the density ( $3.02 \text{ g cm}^{-3}$ ) and the depth of its interfaces remain compatible with the seismic observations. The transitional layer of about 3 km thickness lying between 35 and 38 km depth from the surface along the coast, produced an optimal match. At more than about 40 km from the coastline, a stretched continental crust with a definite amount of high velocity/high density transitional layer is observed.

### Interpretation of the anomalous velocity/density layer

Looking at the presented density models, it is quite obvious that the lower crustal anomalous layer of velocity

$\geq 7.15 \text{ km/s}$  and density  $3.02 \text{ g cm}^{-3}$  plays an important role in crustal evolution along the western part of Indian mainland and adjoining Arabian Sea. Such velocity/density layers are rather unusual in normal crustal structures. They are often found at the crust/mantle boundary in shield regions, in many active rift/graben systems and along passive volcanic continental margins<sup>41</sup>. In the latter regions, the lower crust is altered due to the injection of high-density magmatic material coming from the mantle. Based on the joint (seismic and gravity) data interpretation in the realm of Deccan volcanism, the anomalous layer is attributed to the igneous crustal accretion beneath the region. The delineated crustal structure with under-plated layer is also compatible with the observed lower crustal accretion beneath the adjoining CG (ref. 10).

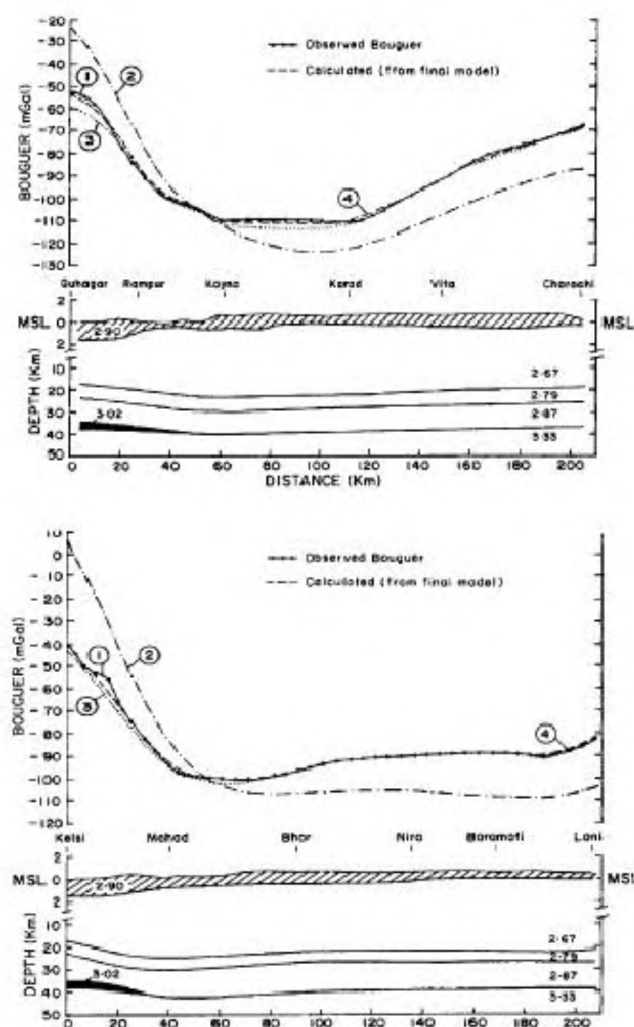


**Figure 9.** 2D density model along Koyana-I and Koyana-II DSS profiles, respectively. Curve 1 is the observed BA, curves 2–4 are the response of the crustal section with the Moho warped up to a depth of 30/31.5 km, with 2 km thick transitional layer lying between 35.5 and 37.5 km depth, and the finally proposed model, respectively. Densities are in  $\text{g cm}^{-3}$ . MSL, mean sea level.



## Supporting geophysical signatures

Genesis of necessary magma responsible for such a large igneous intrusion in the above-mentioned regions has indeed deeper causes; and thermal anomalies due to the intrusion are expected as a result of uprising of partial melt. Interestingly the west-coast megastructure encompassing the CG, the Mumbai offshore region, the Konkan geothermal province and the NTR is characterized by high heat flow and intense distribution of the hot springs (Figure 10; refs 42 and 43). Its manifestation along the west coast is seen as a region of elevated temperature at depths. Murthy<sup>44</sup> assumed that the magma chamber beneath that region has not cooled down completely. For Bose<sup>45</sup> it implies an active mantle at a relatively shallow depth. According to Ravi Shanker<sup>43</sup>, it represents an anomalous hot and/or a zone of intense lower crust and upper mantle interaction. This contention is further corroborated by a 2D magnetovariational study, which has shown that the Satpura range and the west coast of India are the loci of internal current concentration for parts of its length<sup>3</sup>. In view of the known relation between high heat flow and electrical conductivity, it was associated with a partial melt zone in the crust or upper mantle beneath the area of the TJ and under the Satpura ranges<sup>3</sup>. This intra-crustal thermally disturbed layer with high current concentration conforms well to the inferred accreted igneous layer.

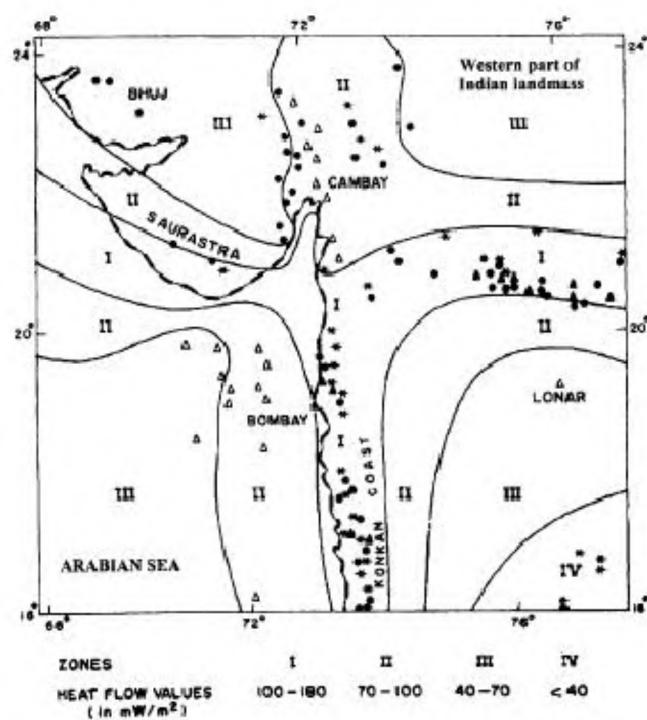


**Figure 10.** Heat-flow map (in  $\text{mW/m}^2$ ) over western India (after Ravi Shanker<sup>43</sup>). Triangles denote published exploratory holes data. Geochemically computed data points are denoted by dots. Stars indicate hot springs.

The present-day high heat flow regime, localization of eruptive centres and basic igneous complexes along the west coast indicate a possible thinning of the lithosphere<sup>46</sup>. In fact, Negi *et al.*<sup>47</sup> found an upwarped asthenosphere in the NTR up to a mean depth of about 57 km. An extremely thinned thermal lithosphere ( $\sim 40$  km) beneath the coastal region indicates a possible presence of partial melting conditions at very shallow depths<sup>17</sup>. The 3D tomographic study further corroborates the contention by revealing a large-scale low-velocity subcrustal zone, which persists till at least 200 km beneath the coastal region of the Deccan volcanic province<sup>48</sup> and adjoining CG (ref. 49). A similar low-velocity fossil mantle plume beneath South America is recently interpreted as the thermal remnant of the original plume conduit that supplied the Parana plume head<sup>50</sup>. The origin and evolution of the inferred crustal accretion beneath the western part of Indian mainland and adjoining Arabian Sea in such a thermally disturbed condition may be seen in the realm of the Deccan magmatism and the Late Cretaceous geodynamics of the Indian subcontinent.

## Geodynamic links

Presence of the accreted igneous layer beneath the region is in agreement with similar observations along the passive volcanic margins all over the world<sup>9,11</sup>. Plausible explanations for the magmatic crustal accretion include plume and non-plume models. With ample independent evidences for a hot spot source for the Deccan magma eruption along the west coast<sup>8,51</sup>, the possible explanation for the present crustal accretion seems to lie in the plume model. According to Meissner<sup>41</sup>, a rising plume of a certain excess temperature diverges laterally in an area with a strong viscosity gradient. Zones of low viscosity, such as the asthenosphere and the continental lower crust, are weak and therefore act as zones of decoupling, attracting lateral movements of the intruding plume material. The tangential stress between laterally moving plume material and the more rigid part of the crust and mantle initiates rifting. On decompression, the plume head with temperature raised to even  $100\text{--}200^\circ\text{K}$  above normal, generates huge amounts of melt<sup>9</sup>. After the extrusion has set in, according to the plume model, no more shear stresses are present and intrusion into the margin decreases. Cooling and contraction leave a rather homogeneous body at the base of the crust. Such a restitic, highly mafic body might have a velocity of  $7.0\text{--}7.5\text{ km s}^{-1}$  on solidifying. It has been predicted that the ponded basaltic melt should have high density ( $2.99\text{--}3.07\text{ g cm}^{-3}$ ) in such regions<sup>9</sup>. Since the density of the generated igneous rock lies midway between that of the mantle and the crust, it explains why a considerable volume of the melt remains trapped as an underplated layer.

Given that the volcanic episode of the Deccan was a consequence of the passage of the northerly-drifting



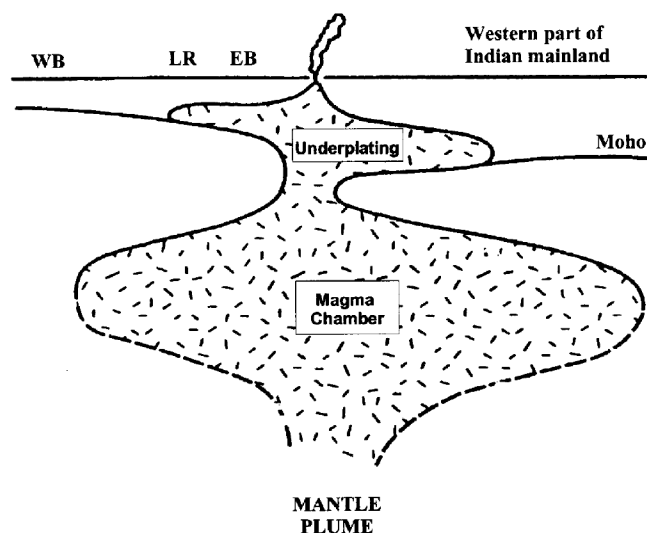


**Figure 11.** Conceptual model of the lithospheric structure beneath the western part of Indian mainland and adjoining Arabian Sea. Present-day configuration with the inherited temperature and density anomalies due to ascending mantle plume beneath the study area is shown.

Indian subcontinent over the Reunion starting plume, the conspicuous concentration of plutonic bodies and volcanic plugs around the TJ presents itself as a potential site for the lava eruption. Before extrusion, the Deccan plume head mushrooming beneath the region probably found a low viscosity environment leading to huge magmatic intrusion in the western part of Indian mainland and adjoining Arabian Sea. The conceptual model presented in Figure 11 gives a general idea of the ascending mantle plume, the asthenospheric magma accumulation, igneous crustal accretion and subsequent extrusion of Deccan flood basalts about 65 MaBP. On the basis of the plume trace, it has been suggested that after the major hot spot outburst close to the TJ, the trail of the plume moved into the ocean near Koyna<sup>12</sup>. The inferred crustal accretion, about 3 km thick and 40 km wide, in the Konkan coastal region is possibly the imprint of the subsequent magmatic intrusion in a similar environment during the northward migration of the Indian subcontinent over the Reunion hot spot.

## Conclusions

Based on the seismic evidence and extensive gravity modelling, this study thus postulates the presence of a large-scale crustal accretion along the western part of Indian mainland and adjoining Arabian Sea, similar to that seen along the other volcanic continental margins of the world. The greater thickness of the accreted igneous layer beneath the Navsari gravity high presents itself as one of the potential sites for the Deccan magma evolu-

tion. The study further brought out a normal oceanic crustal structure followed by an accreted igneous layer at the base of the crust beneath the LR. The conceptual model provides the right kind of geometrical configuration for the crustal accretion beneath the region. The locus of the plume path predicts the subsequent crustal accretion beneath the Koyna coastal region in the moving plate environment.

1. NGRI 1978 NGRI/GHP-1 to 5, Gravity Maps of India, scale 1 : 5,000,000; National Geophysical Research Institute, Hyderabad.
2. Saxena, V. K. and Gupta, M. L., *J. Volcanol. Geotherm. Res.*, 1987, **33**, 337–342.
3. Arora, B. R. and Reddy, C. D., *Phys. Earth Planet. Inter.*, 1991, **66**, 118–131.
4. Cox, K. G., *Nature*, 1989, **342**, 873–877.
5. Burke, K. and Dewey, J. F., *J. Geol.*, 1973, **81**, 406–433.
6. Courtillot, V., Feraud, G., Maluski, H., Vandamme, D., Moreau, M. G. and Besse, J., *Nature*, 1988, **333**, 843–846.
7. Duncan, R. A. and Pyle, D. G. *ibid.*, 841–843.
8. Richards, M. A., Duncan, R. A. and Courtillot, V. E., *Science*, 1989, **246**, 103–107.
9. White, R. S. and McKenzie, D. P., *J. Geophys. Res.*, 1989, **94**, 7685–7729.
10. Kaila, K. L. and Krishna, V. G., *Curr. Sci.*, 1992, **62**, 117–154.
11. Coffin, M. F. and Eldholm, D., *Rev. Geophys.*, 1994, **32**, 1–36.
12. Raval, U., *PAGEOPH*, 1995, **145**, 175–192.
13. Kaila, K. L. and Sain, K., *J. Geol. Soc. India*, 1997, **49**, 395–407.
14. Bhattacharji, S., Chatterji, N., Wampler, J. M., Nayak, P. N. and Deshmukh, S. S., *J. Geol.*, 1996, **104**, 379–398.
15. Auden, J. B., *Trans. Natl. Inst. Sci. India*, 1949, **3**, 123–157.
16. Qureshy, M. N., *J. Geophys. Res.*, 1971, **76**, 545–557.
17. Negi, J. G., Agrawal, P. K., Singh, A. P. and Pandey, O. P., *Tectonophysics*, 1992, **206**, 341–350.
18. Verma, R. K. and Banerjee, P., *Tectonophysics*, 1992, **202**, 375–397.
19. Singh, A. P. and Meissner, R., *J. Geodyn.*, 1995, **20**, 111–127.
20. Singh, A. P., *J. Geodyn.*, 1998, **25**, 129–141.
21. Jacobsen, B. H., *Geophysics*, 1987, **52**, 1138–1148.
22. Götte, H. J. and Lahmeyer, B., *Geophysics*, 1988, **53**, 1096–1108.
23. Naini, B. R. and Talwani, M., *Am. Assoc. Petrol. Geol. Mem.*, 1982, **34**, 167–191.
24. Kolla, V. and Coumes, F., *Mar. Petrol. Geol.*, 1990, **7**, 188–196.
25. Pandey, O. P., Agrawal, P. K. and Negi, J. G., *Geo-Mar. Lett.*, 1995, **15**, 85–91.
26. Bhattacharya, G. C., Chaubey, A. K., Murthy, G. P. S., Srinivas, K., Sarma, K. V. L. N. S., Subrahmanyam, V. and Krishna, K. S., *Earth Planet. Sci. Lett.*, 1994, **125**, 211–220.
27. Singh, A. P., *J. Geodyn.*, 1999, **27**, 609–622.
28. Liu, C. S., Sandal, D. T. and Curry, J. F., *J. Geophys. Res.*, 1982, **87**, 7673–7686.
29. Jonas, J., Hall, S. and Casey, J. F., *J. Geophys. Res.*, 1991, **96**, 759–777.
30. Krishna Brahman, N. and Negi, J. G., *Geophys. Res. Bull.*, 1973, **2**, 207–237.
31. Kailasam, L. M., Murty, B. G. K. and Chayanulu, A. Y. S. R., *Curr. Sci.*, 1972, **45**, 9–13.
32. Mishra, D. C., *J. Geol. Soc. India*, 1989, **33**, 48–54.

- 
33. Gokaran, S. G., Rao, C. K., Singh, B. P. and Nayak, P. N., *Phys. Earth Planet. Inter.*, 1992, **72**, 58–67.
34. Subrahmanyam, C. and Verma, R. K., *Tectonophysics*, 1980, **69**, 147–162.
35. Qureshy, M. N., *Geol. Soc. India Mem.*, 1981, **3**, 184–197.
36. Takin, M., *Geophys. J. R. Astron. Soc.*, 1966, **11**, 527–537.
37. Chandrasekharam, D., *Phys. Earth Planet. Inter.*, 1985, **41**, 186–198.
38. Mishra, D. C., Gupta, S. B. and Tiwari, V. M., *Int. Geol. Rev.*, 1999, **40**, 1007–1020.
39. Singh, A. P. and Mall, D. M., *Tectonophysics*, 1998, **290**, 285–297.
40. Krishna, V. G., Kaila, K. L. and Reddy, P. R., *AGU Geophys. Monogr.*, 1989, **51**, 143–157.
41. Meissner, R., *The Continental Crust: A Geophysical Approach*, Academic Press, New York, 1986.
42. Krishnaswamy, V. S. and Ravi Shanker, *Rec. Geol. Surv. India*, 1980, **111**, 17–40.
43. Ravi Shanker, *Indian Miner.*, 1988, **42**, 89–110.
44. Murthy, M. V. N., *Geol. Soc. India Mem.*, 1981, **3**, 93–100.
45. Bose, M. K., *Lithos*, 1972, **5**, 131–145.
46. Biswas, S. K., *Am. Assoc. Petrol. Geol.*, 1982, **66**, 1497–1513.
47. Negi, J. G., Pandey, O. P. and Agarwal, P. K., *Tectonophysics*, 1986, **131**, 147–156.
48. Ramesh, D. S., Srinagesh, D., Rai, S. S., Prakasam, K. S. and Gaur, V. K., *Phys. Earth Planet. Inter.*, 1993, **77**, 285–296.
49. Kennett, B. L. N. and Widiyantoro, S., *Earth Planet. Sci. Lett.*, 1999, **165**, 145–155.
50. Van-Decar, J. C., James, D. E. and Assumpcao, M., *Nature*, 1995, **378**, 25–31.
51. Morgan, W. J., *Am. Assoc. Petrol. Geol. Bull.*, 1972, **56**, 203–213.
- ACKNOWLEDGEMENTS. I thank the Director, National Geophysical Research Institute, Hyderabad for his kind permission to publish this work. Thanks are also due to the anonymous reviewer for useful suggestions.
- Received 19 May 2001; revised accepted 9 October 2001
-